Supporting Information for Unravelling nonlinear spectral evolution using nanoscale photonic near-field point-to-point measurements

Matthias Wulf,* Daryl M. Beggs, Nir Rotenberg, and L. Kuipers

Center for Nanophotonics, FOM Institute for Atomic and Molecular Physics (AMOLF), Science Park 104, 1098XG, Amsterdam, The Netherlands

E-mail: wulf@amolf.nl

Sample details

The photonic crystal (PhC) consists of a 220 nm thick silicon membrane which is perforated with air holes. The holes have a radius of 0.29a and are periodically arranged in a triangular lattice ($a = 420\,nm$). One row of holes is not present in the $\Gamma - K$ crystal direction, creating the waveguide. The sample was fabricated by electron beam lithography, subsequent dry etching and sacrificial wet etching to release the membrane.[1] The two rows of holes directly adjacent to the waveguide are shifted by -0.11a and 0.06a, respectively, to create a spectral slow light regime with low group velocity dispersion.[2] A negative shift is defined here as a displacement from the position dictated by the triangular lattice towards the waveguide and a positive shift as a displacement away from the waveguide.

The light injection from a ridge waveguide to a slow light photonic crystal can be very inefficient due to an increasing mode mismatch with increasing n_g. In our experiment, this mismatch

*To whom correspondence should be addressed

would result in inefficient in- and outcoupling for wavelengths above 1577 nm. To overcome this problem we have changed the lattice constant of the first and last ten periods of our photonic crystal to a value of 440 nm which shifts the whole bandstructure to longer wavelengths. This shift creates a photonic crystal with $n_g = 5$ across the entire spectrum of our laser, which acts as an interface between the ridge waveguide and the slow light PhC. It has been shown in literature that this gradual approach of first exciting a fast light mode, which then couples to a slow mode, is very efficient and can lead to injection efficiencies above 90 % for group indices up to 100.[3]

Broadening of the transmission spectra

The width of a spectrum can be quantified by calculating its second moment, i.e. variance σ, which is defined by

$$\sigma^2 = \frac{\int (\overline{\lambda} - \lambda)^2 \, P(\lambda) \, d\lambda}{\int P(\lambda) \, d\lambda}. \tag{1}$$

where $\overline{\lambda}$ is the first moment, i.e. mean wavelength, as defined in Eq. (1) in the maintext.

The change of the spectral width, which is the square root of the variance, of the transmission spectra with input power is shown in Supporting Figure 1. It is obvious that the spectra get broader with increasing input power. By going from 1.1 mW to 25.8 mW the spectral width nearly doubles from 7 nm to 12 nm.

Details of the modeling approach

To model the pulse propagation through the PhC waveguide Eq. (2) and Eq. (4) of the maintext are solved by means of the split-step Fourier method.[4] The temporal evolution of free-carrier density N_c is calculated by solving Eq. (3) of the maintext with a first-order finite-difference scheme.[5]

We fit our model to the measured pulse evolution by adjusting only two parameters: a simple scaling factor modeling the near-field probe pickup-efficiency, and a number that describes the

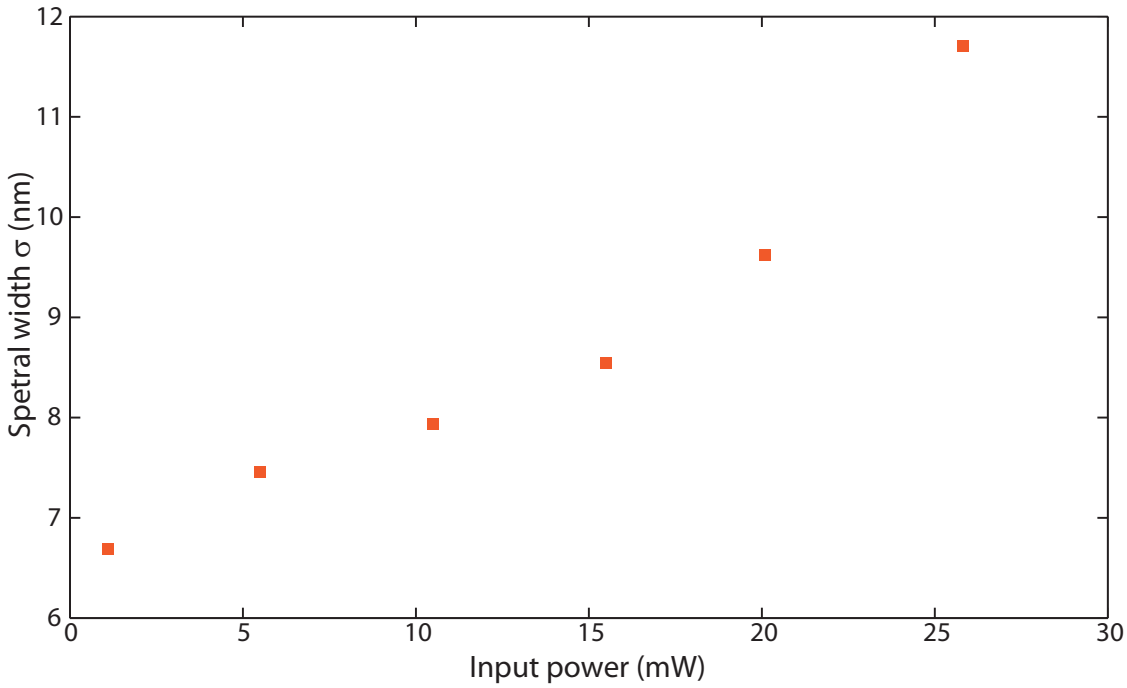

Supporting Figure 1: Spectral width of the transmission spectra shown in figure 2a in the maintext for different average input powers.

chirp the pulse experiences in the polymer access waveguide and the silicon spot-size converter. This latter parameter determines the temporal length of the pulse at the beginning of the PhC waveguide. As starting conditions the first spectrum taken at the beginning of the PhC waveguide and the free-carrier density N_c are set to zero. The best agreement between the model and the experimental results is achieved with a temporal length of 1.38 ps (FWHM). This amount of temporal broadening is reasonable considering the few millimeter distance that the pulse has to propagate through the sample before it enters the PhC waveguide. The blueshift of the spectral density, which occurs either inside the polymer access waveguide or the silicon spot-size converter, is taken into account in the modeling by shifting the centre frequency of the pulse in a one-time fit to the spectrum measured at the beginning of the PhC (cf. Figure 3d of the maintext).

The effective values of all wavelength-dispersive parameters used for simulating the propagation of the different spectral components, shown in Figure 4 of the main text, are presented in Supporting Table 1. The intrinsic material dispersion is negligible over the considered wavelength range. Thus, the observed wavelength dependency arises solely from the photonic crystal induced

dispersion of the slowdown factor S and its influence on the various parameters (see Table 1 in the main text).

The scaling of the linear loss with the slowdown factor is nontrivial, because it consists of both backscattering and out-of-plane scattering, which have different S dependencies. In our modelling we have assumed that the linear losses are dominated by out-of-plane scattering, which is typically for moderate group indices (e.g. $n_g < 50$, depending on the PhC design).[6] Consequently, α_{eff} increases linearly with S.

Supporting Table 1: The effective of all wavelength-dispersive parameters used in the simulation. These values are inclusive of the slowdown enhancement.

Free-space wavelength	$\alpha_{eff}(dB/cm)$	$\beta_{eff}(cm/GW)$	$n_{2,eff}(cm/W)$	$\sigma_{eff}(m^2)$	$k_{c,eff}(m^3)$
1565 nm	22.93	3.97	$2.38 \cdot 10^{-13}$	$2.89 \cdot 10^{-21}$	$2.69 \cdot 10^{-27}$
1575 nm	27.09	26.24	$1.57 \cdot 10^{-12}$	$7.43 \cdot 10^{-21}$	$6.92 \cdot 10^{-27}$
1580 nm	31.78	227.48	$1.36 \cdot 10^{-11}$	$2.19 \cdot 10^{-20}$	$2.04 \cdot 10^{-26}$

Error due to change of transversal field profile

As mentioned in the maintext there is a positional accuracy in placing the near-field probe always at a single position inside a unit cell of the PhC waveguide throughout the measurements. As a consequence, we observe an artificial amplitude modulation in the spectra taken by means of the SNOM. To quantify the possible variation of the signal, we simulate the intensity of the mode inside the PhC waveguide by using MIT Photonics Band Package (MPB).[7] We convolute the calculated intensity profile with a circle of 250 nm to mimic the effect of the aperture size of the near-field probe. The results for the three wavelengths, which are also investigated and modeled in the maintext, are shown in Supporting Figure 2a)-c).

Since we scan the near-field probe transversally over the PhC waveguide to counteract the different extension of the mode profiles visible in the MPB calculations, we integrate the simulated intensity distribution over the x-axis resulting in sinus curves with different modulation depths as shown in Supporting Figure 2d)-f). The error bars, used in Figure 4 in the maintext, are calculated

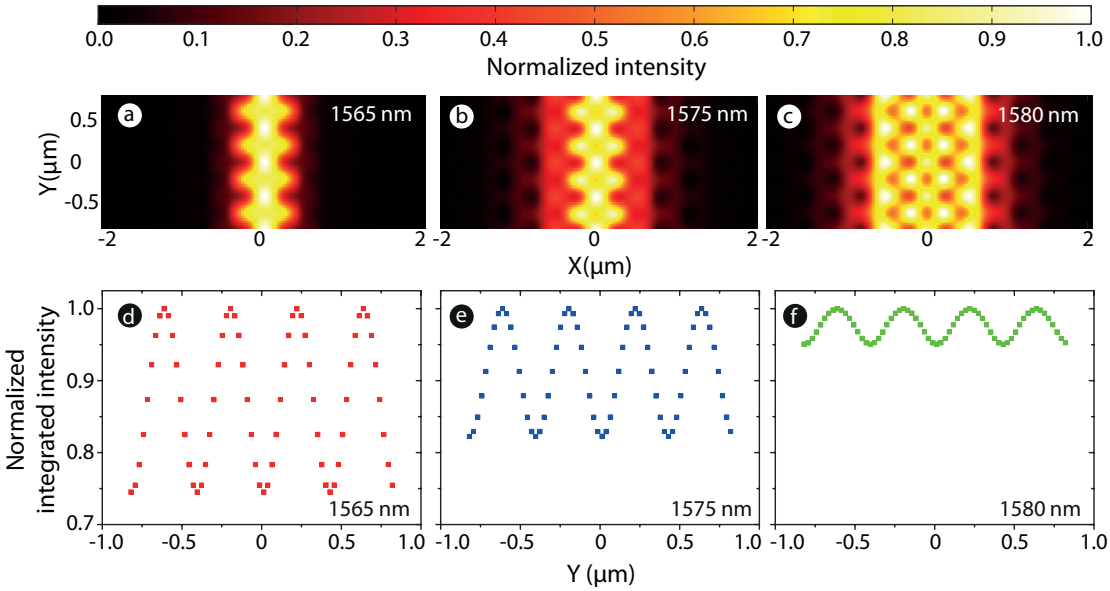

Supporting Figure 2: Calculated intensity distribution convoluted with a 250 nm diameter circle for a wavelength of (a)1565 nm, (b)1575 nm and (c)1580 nm for four unit cells of the PhC waveguide. Corresponding transversally integrated intensity curves.

by determining the ratio of the standard variation to the mean value of these integrated intensity curves, which are listed in Supporting Table 2. It is clear that the intensity profile at the shortest wavelength features the biggest modulation along the propagation direction leading to the largest error bar. For increasing wavelength, the modulation decreases.

Supporting Table 2: Table containing the mean value, standard variation and their ratio for the curves shown in Supporting Figure 2d)-f).

Wavelength	Mean	Standard variation	Ratio
1565 nm	0.87	0.09	10.38 %
1575 nm	0.91	0.063	6.93 %
1580 nm	0.98	0.018	1.8 %

As mentioned in the maintext, the 2 % error bar calculated for the wavelength 1580 nm is too small (cf. Figure 4 in maintext). We attribute this discrepancy to the slow group velocity that the mode inside the PhC waveguide experiences at this wavelength. The slow light enhancement leads to an increased sensitivity of the guided light to possible perturbations. Thus, we estimated an increased background noise level leading to an error bar of 5 %.

References

(1) Reardon, C. P.; Rey, I. H.; Welna, K.; O'Faolain, L.; Krauss, T. F. *J Vis Exp.* **2012**, *69*, E50216.

(2) Li, J.; White, T. P.; O'Faolain, L.; Gomez-Iglesias, A.; Krauss, T. F. *Opt. Express* **2008**, *16*, 6227–6232.

(3) Hugonin, J. P.; Lalanne, P.; White, T. P.; Krauss, T. F. *Opt. Lett.* **2007**, *32*, 2638–2640.

(4) Sinksen, O. V.; Holzlöhner, R.; Zweck, J.; Menyuk, C. R. *J. Lightwave Technol.* **2003**, *21*, 61–68.

(5) LeVeque, R. J. *Finite Difference Methods for Ordinary and Partial Differential Equations*; Society for Industrial and Applied Mathematics, 2007.

(6) O'Faolain, L.; Schulz, S. A.; Beggs, D. M.; White, T. P.; Spasenović, M.; Kuipers, L.; Morichetti, F.; Melloni, A.; Mazoyer, S.; Hugonin, J. P.; Lalanne, P.; Krauss, T. F. *Opt. Express* **2010**, *18*, 27627–27638.

(7) Johnson, S.; Joannopoulos, J. *Opt. Express* **2001**, *8*, 173–190.